Experimental and theoretical study of electronic structure of lutetium bi-phthalocyanine

I. Bidermane, J. Lüder, S. Boudet, T. Zhang, S. Ahmadi et al.

Citation: J. Chem. Phys. **138**, 234701 (2013); doi: 10.1063/1.4809725
View online: http://dx.doi.org/10.1063/1.4809725
View Table of Contents: http://jcp.aip.org/resource/1/JCPSA6/v138/i23
Published by the AIP Publishing LLC.

Experimental and theoretical study of electronic structure of lutetium bi-phthalocyanine

I. Bidermane,[1,2,a)] J. Lüder,[1] S. Boudet,[3] T. Zhang,[2] S. Ahmadi,[4] C. Grazioli,[5] M. Bouvet,[6] J. Rusz,[1] B. Sanyal,[1] O. Eriksson,[1] B. Brena,[1] C. Puglia,[1] and N. Witkowski[2]
[1]*Department of Physics and Astronomy, Uppsala University, Box-516, 75120 Uppsala, Sweden*
[2]*Institut des Nanosciences de Paris, UPMC Univ. Paris 06, CNRS UMR 7588, F-75005 Paris, France*
[3]*Laboratoire de Projection Thermique, CEA Le Ripault, Département Matériaux, 37260 Monts, France*
[4]*Materialfysik, KTH-Electrum, Isafjordsgatan 22, 16440 Kista, Sweden*
[5]*Sincrotrone Trieste S.C.p.A., Area Science Park, S.S.14, Km 163.5, 34012 Trieste, Italy*
[6]*Institut de Chimie Moléculaire de l'Université de Bourgogne, CNRS UMR 6302, Université de Bourgogne, F-21078 Dijon, France*

(Received 19 March 2013; accepted 23 May 2013; published online 17 June 2013)

Using Near Edge X-Ray Absorption Fine Structure (NEXAFS) Spectroscopy, the thickness dependent formation of Lutetium Phthalocyanine ($LuPc_2$) films on a stepped passivated Si(100)2×1 reconstructed surface was studied. Density functional theory (DFT) calculations were employed to gain detailed insights into the electronic structure. Photoelectron spectroscopy measurements have not revealed any noticeable interaction of $LuPc_2$ with the H-passivated Si surface. The presented study can be considered to give a comprehensive description of the $LuPc_2$ molecular electronic structure. The DFT calculations reveal the interaction of the two molecular rings with each other and with the metallic center forming new kinds of orbitals in between the phthalocyanine rings, which allows to better understand the experimentally obtained NEXAFS results. © *2013 AIP Publishing LLC*. [http://dx.doi.org/10.1063/1.4809725]

I. INTRODUCTION

Hybrid systems are experiencing an unprecedented development for the fabrication of devices in various sectors of nanotechnology. In such a context, phthalocyanine (Pc) complexes have received a great deal of attention because of their unique optical and electronic properties and high thermal stability. Many relevant applications have emerged such as energy cells,[1] electrochromic displays,[2] and gas sensors.[3,4] This rapid development leads to the need of deep investigations and comprehensive understanding of molecule/substrate interface formation in the initial growth phase and molecule/molecule interaction in the next phases. Electron spectroscopies, such as X-ray Photoemission Spectroscopy (XPS) and Near Edge X-ray Absorption Fine Structure Spectroscopy (NEXAFS) can provide direct information on the bonding between Pc and the substrate and the electronic charge distribution and the geometric configuration (arrangement of the adsorbed molecules).

Recently, rare-earth double-decker phthalocyanine molecules have attracted a great attention for their application in organic-based field effect transistors[5,6] due to their tunable electronic properties. In this study, we focus on double-decker lutetium phthalocyanine ($LuPc_2$), which is composed of two identical phthalocyanines, rotated by 45° against each other and bridged via a Lu(III) ion as depicted in Fig. 1. The electronic structure of $LuPc_2$ is characterized by a single semi-occupied molecular orbital (SOMO) between the highest occupied molecular orbital (HOMO) and the lowest unoccupied molecular orbital (LUMO), i.e., in the HOMO-LUMO gap. Therefore, the SOMO electronic state can accommodate or donate its electron, making $LuPc_2$ a tunable donor or acceptor carrier transporter.

Despite a very large amount of work devoted to the elucidation of molecular interaction of Pc molecules on metal surfaces,[7,8] only few studies have focused on the semiconducting surfaces[9,10] and even less on double-decker Pc's on these technologically relevant surfaces.[11,12] On most metallic surfaces, Pc molecules are known to lie flat, whereas the molecular architectures are various on semiconducting substrates. Pc molecules are found lying flat on InSb(001) surface,[9] whereas they are inclined on Si(001).[11,13] Furthermore, a transition from lying-down to standing-up configuration occurs in less than one monolayer of CuPc on Si(111).[14] The different orientations are also observed on passivated surfaces. PbPc molecules are found to be flat on passivated Ge,[15] whereas CuPc molecules are standing up on Si(001) passivated with H or NH_3.[16] In this context, the orientation of $LuPc_2$ adsorbed on the passivated Si(100)-2×1:H is here investigated by means of synchrotron based techniques, such as XPS and NEXAFS, in combination with DFT calculations.

We show that $LuPc_2$ has a weak chemical interaction with the substrate. In this sense, our study can be considered as a comprehensive study of the electronic structure of the $LuPc_2$ molecules. Our results elucidate the different electronic structure of double decker phthalocyanines compared to single decker phthalocyanines using experimental NEXAFS measurements supported by the DFT calculations. We also find a change in the orientation of the molecules as a function

a)Electronic mail: ieva.bidermane@physics.uu.se

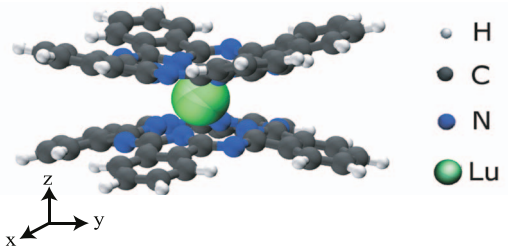

FIG. 1. $LuPc_2$ structure optimized by DFT calculations.

of coverage and derive an average tilt angle from the DFT calculations.

II. EXPERIMENTAL DETAILS

Experiments have been carried out at the Swedish national synchrotron MAX-Lab on two beamlines – beamline I511 surface branch-line and D1011 beamline, as well as at the French national synchrotron SOLEIL on the beamline TEMPO.

A. Sample preparation

Single-domain vicinal n-doped Si(001), provided by Siltronix, with a 4° miscut angle in [110] direction was prepared using a standard procedure already described in previous works.[17,18] In order to reduce the interaction between the substrate and the organic layer, required for a comprehensive molecular electronic structure investigation, the silicon surface was passivated by a hydrogenation process, i.e., passivating the silicon surface atoms (dangling bonds) by hydrogen atoms.[19] The hydrogenation was performed using an Omicron Atomic Hydrogen Source at the I511 end-station and D1011 beam line, and a hot filament located few centimeters from the surface of the sample at TEMPO beamline. The pressure during the hydrogenation was kept in the mid 10^{-8} mbar range, while setting the Si surface at 300 °C, leading to a 2×1 reconstruction as checked with Low Energy Electron Diffraction (LEED).

$LuPc_2$ was synthesized according to the literature methods.[20] Knudsen cell type evaporator from Ferrovac was used to evaporate $LuPc_2$, which was outgassed for few hours at 250 °C until recovering the base pressure (low 10^{-10} mbar range). During the molecular deposition, the crucible was heated resistively around 300 °C, while keeping the vapor pressure in the 10^{-9} mbar range. Several samples have been prepared with varying thicknesses from submonolayer up to several layers.

The thicknesses of organic films (from monolayer up to bulk like film) were estimated from photoemission spectroscopy data using a so-called overlayer method,[21] assuming exponential decay of the substrate core level intensity.

B. XPS measurements

The experiment was carried out at TEMPO beamline at the French synchrotron facility (SOLEIL) in France. TEMPO is a soft x-rays beamline that can produce radiation with any orientation of circular and linear polarization with photon energy ranging from 50 eV to 1500 eV. The beamlines end station is equipped with a Scienta-200 electron analyzer dedicated to electron spectroscopy studies of surfaces. Details on the TEMPO beamline and its end-station can be found in Ref. 22.

Core level XPS spectra were taken in normal emission of the photoelectrons. Photon energies of 160 eV and 330 eV were used for Si 2p and C 1s core levels, respectively. The overall resolution of core level spectra was about 50 meV. Shirley background has been removed from all XPS spectra[23] and, height has been normalized to unity on the largest peak. The binding energy (BE) has been calibrated with respect to the Si $2p_{3/2}$ bulk component set at 99.35 eV in BE, as found in the literature.[24]

C. NEXAFS measurements

The experiments were performed at beamlines I511 at the MAX-Lab synchrotron radiation facility in Lund, Sweden. I511 is an undulator based beamline with a Zeiss SX700 plane grating monochromator providing high-intensity linearly polarized synchrotron radiation of the photon energy ranging from 100 to 1500 eV. The end station was equipped with Scienta R4000 hemispherical electron energy analyzer and the analysis chamber could be rotated around the incoming beam. Additional details about experimental set-up can be found in Ref. 25.

Absorption spectra of nitrogen were recorded in Auger electron yield mode in an energy window of 30 eV around the nitrogen KLL transition at 370 eV, the incoming photon energy ranging from 395 eV to 425 eV. Electrons were detected in a 45° angle with respect to the polarization vector. The spectra were first normalized to the intensity of the incoming light measured on a gold mesh, then normalized to unity at 425 eV.[26] Two polarizations were investigated: in-plane polarization (IPL) for which the polarization E vector of the radiation was parallel to the surface and out-of-plane polarization (OPL) for which the polarization was about 83° from the surface plane. The photon energy calibration was done by measuring the first and second order light from the Si 2p core level for thin layers, and C 1s core level spectra for thick layers. The overall resolution of NEXAFS spectra is about 100 meV. Due to poor statistics for thin layer measurements obtained on I511, data from another experiment performed on D1011 (Max-Lab) on the same system were used, taking care that the overall line shape of both spectra was identical.

III. COMPUTATIONAL DETAILS

The ground state calculation and geometry optimization of $LuPc_2$ were performed by means of DFT calculations using the GAUSSIAN 09 program[27] with the hybrid UB3LYP exchange-correlation functional.[28] The lutetium atom was described by the Dresden/Stuttgart effective core potential (SDD) basis set[29] and all the other atoms by the 6-31G(d,p) valence double ζ plus polarization basis set. It has to be noted

that the full relaxation of the $LuPc_2$ does not result in a structure as flat as the one previously obtained by x-ray diffraction by De Cian *et al.*,[30] as also observed in previous theoretical studies.[31]

The DFT optimized structure is shown in Fig. 1. It belongs formally to the C_{4v} point group. The experimental molecular structure by De Cian *et al.*[30] and the one shown in Fig. 1 differ mainly in the bending of the isoindole rings. Unlike the X-ray diffraction structure,[30] the DFT optimized structure shows a distortion of the phthalocyanine rings away from the molecular center, bending by an angle of about 13 °. Including the van der Waals correction by using the CAM-B3LYP[32] functional, the bending of the molecule could be reduced by 2 °. The influence of the dispersion correction on the intra-molecular structure is small and the differences between the experimental X-ray diffraction structure and the DFT optimized structure can most likely be related to the missing inter-molecular forces in the mentioned single molecule calculations. Therefore, the B3LYP optimized structure is an appropriate approximation for the sub-monolayer molecular structure of $LuPc_2$ at a weakly reactive surface. Both, the experimental X-ray diffraction and the DFT optimized, structures have the rings rotated by 45 ° with respect to each other, sandwiching a lutetium atom.

To simulate the N 1s NEXAFS spectra, we have applied the transition-potential approach (TPA)[33–35] used in the DFT code WIEN2K to a geometry optimized molecule.[36] In a TPA calculation, the electronic relaxation effects induced by the transition of an electron from an initial to a final state are simulated by the introduction of a half core hole at a particular core level. In the case of $LuPc_2$, two spin polarized TPA calculations, one for each non-equivalent nitrogen atom, were performed. 12 871 basis functions were used to describe the orbitals for each spin population within the full-potential linearised-augmented-plane-wave method (FP-LAPW). The radii of the muffin-tin spheres of each atom kind can be found in Table I.

Valence and core states were separated at the energy of −6.0 Rydberg (Ry). Core level charge density leaking out of the muffin tin spheres was of negligible amount. The generalized gradient approximation (GGA) exchange-correlation functional by Perdew-Burke-Ernzerhof (PBE) was used.[37] The dimension of the unit cell was 39 × 39 × 18 Å in the x, y, and z directions, respectively. A uniform background charge of half an electron was added to the unit cell for charge neutrality. Since a single molecule is considered, only the gamma point in the Brillouin zone was sampled. The C_4-fold rotation axis of the $LuPc_2$ was aligned parallel to the z direction of the unit cell, which in our convention represents a molecule adsorbed parallel to the surface.

TABLE I. Muffin tin sphere radii for different kinds of atoms in the TPA calculation.

	Inner shell radius (bohrs)
Lu	2.28
N	1.20
C	1.20
H	0.8

To simulate the polarization resolved X-ray absorption spectra, we have considered the partial density of states (pDOS) of unoccupied p-orbitals (i.e., the orbitals with energies above the HOMO) for each of the two non-equivalent nitrogen atoms. The projections of the pDOS along the three spatial coordinates x, y, and z correspond to the intensities of the spectra along the same directions: I_x, I_y, and I_z. The optimized geometry of $LuPc_2$ molecule is shown in Fig. 1. When it is adsorbed parallel to the surface, the in-plane components I_x and I_y represent the electron excitations into the unoccupied σ-states, collectively indicated as I_σ, whereas the out-of-plane component I_z, orthogonal to the molecular plane, represents the excitations into the unoccupied π-states, indicated as I_π. In the comparison with the experimental NEXAFS, we need to consider additionally the possible tilting of the adsorbed molecules with respect to the surface plane. When the molecule is tilted, the results of the measurements cannot be compared with pure theoretical I_π and I_σ. The tilt angle can, however, be simulated in the calculations by assuming an angle θ between the C_4-fold axis of the molecule and the z axis of our reference system. Due to the orthogonality of the components I_x, I_y, and I_z, the pDOS of a tilted molecule is obtained as a superposition of I_σ and I_π with the angle θ as a parameter. The total spectrum of a molecule tilted by θ can thus be expressed as the sum of $I_\pi \cos^2(\theta)$ and $I_\sigma \sin^2(\theta)$ where I_π is equal to I_z and I_σ is equal to $0.5 \cdot (I_x + I_y)$. The I_π and I_σ intensities correspond to tilt angles θ equal to 0 ° and 90 °, respectively. The total N 1s spectrum was aligned to the experimental energy scale. To facilitate the comparison with the experiment, the pDOS was convoluted with a Gaussian curve. We used a Gaussian with a full width at half maximum (FWHM) of 0.35 eV below 399 eV, a linearly increasing FWHM from 0.35 to 1.7 eV up to 413.9 eV, and a constant FWHM of 1.7 eV above 413.9 eV.

IV. RESULTS AND DISCUSSION

In this section, we first present the experimental part, where the characteristics of the studied system will be described in comparison with previous studies performed on similar materials. This part is followed by the results obtained from our theoretical calculations, where we will focus on the atomic contribution to the molecular electronic structure and on the orientation of the molecules in overlayers of different thicknesses.

A. XPS data analyses

Si 2p XPS spectra recorded for an excitation energy of 160 eV are displayed in Fig. 2; all spectra have been normalized to unity at the main peak. Si 2p on clean silicon (red line), identical to previously published spectra on stepped surface,[38] presents a pronounced surface state at lower binding energy that characterizes a clean and well reconstructed (100)-2 × 1 vicinal surface. After hydrogenation, the Si dangling bonds have been terminated with hydrogen and

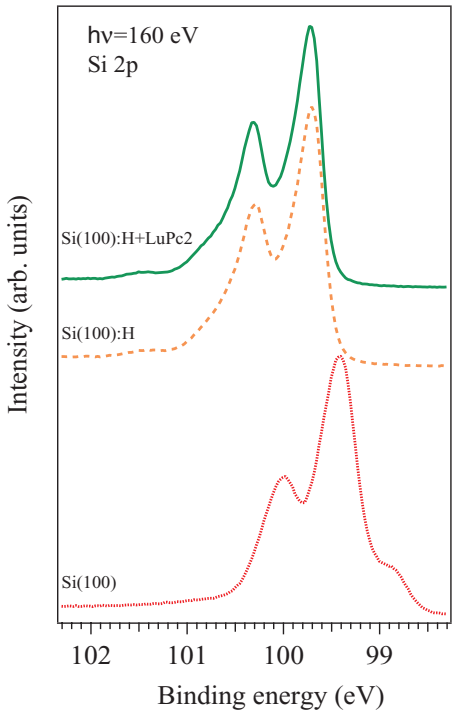

FIG. 2. Silicon 2p XPS spectra recorded for a photon energy of 160 eV: clean silicon (100)-2 × 1 vicinal surface (red line); hydrogenated silicon (100)-2 × 1 vicinal surface (orange dashed line); 0.2 nm of $LuPc_2$ on hydrogenated silicon (100)-2 × 1 vicinal surface (green line on top).

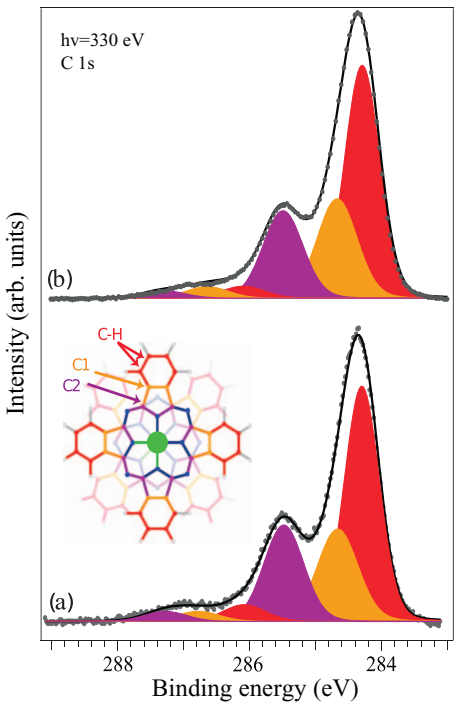

FIG. 3. C 1*s* XPS spectra recorded for photon energy of 330 eV on $LuPc_2$ deposited on hydrogenated silicon (100)-2 × 1 vicinal surface: (a) 1 nm; (b) bulk $LuPc_2$; decomposition with Gaussian function is displayed for each spectra.

therefore no surface states are visible in the spectrum (orange dashed line Fig. 2). The general spectral shape is also modified and is similar to the one already published.[39] Moreover, the spectrum presents an energy shift of 0.3 eV to higher binding energy, commonly attributed to a band bending due to the charge transfer between adsorbed hydrogen atoms and silicon.[38] The small feature at around 101.4 eV is characteristic of a Si^{2+} oxidation state[40] and is attributed to a slight water contamination during the hydrogenation process. The green line corresponds to 0.2 nm of $LuPc_2$ deposited on the hydrogenated surface. The overall shape of the spectrum is identical to the hydrogenated one and no additional features, which could be an indication of a bonding between the molecules and the silicon, are visible. This supports the fact that the passivated Si surface does not interact significantly with the $LuPc_2$ molecules.

Figure 3 displays the C 1s spectra recorded for a thin film of 1 nm (a) and for a thick film deposition (b) on the H-terminated Si surface. The binding energy of the main structure is found at the same position as in previously published XPS on $LuPc_2$ thick film on silver[41] and no energy shift is observed for the different thicknesses, indicating equivalent interaction for the thin and thick layers, a consequence of the Si surface passivation.

The C 1s XPS spectra provide further evidence of the negligible interaction between the adsorbed molecules and the silicon atoms. The spectra can be decomposed using Voigt functions into a series of six peaks. The three larger peaks at lower binding energies corresponding to inequivalent carbons (illustrated in the sketch of Figure 3) are found, respectively, at 284.29 eV for the C-H contribution, 284.66 eV for the C1 contribution, and 285.48 eV for the C2 contribution. The three smaller additional features at higher binding energies correspond to the shake-up transitions associated with the three main transitions C-H, C1, and C2. Shake-up satellites are identified at higher binding energies (i.e., lower kinetic energy) due to a kinetic-energy loss of photoelectrons via simultaneously excited $\pi - \pi^\star$ transitions. Fitting parameters are found in Table II.

The intensity ratio is found to be 1.9 : 1.9 : 4 (C1+shake-up : C2+shake-up : CH+shake-up) for the 1 nm layer and 2.1 : 1.76 : 4 (C1+shake-up : C2+shake-up : CH+shake-up) for the bulk layer. The C2 intensity ratio is smaller than 2 due to a slight beam damage of the layer. The overall ratios are in very good agreement with the numerical ratio of distinct types of carbon atoms identified within the molecular ligand 2 : 2 : 4 (C1+shake up : C2+shake up : CH+shake-up).

TABLE II. Fitting parameters for 1 nm thick and bulk films, FWHM corresponds to the full width at half maximum of the Voigt curve.

	Position (eV)		FWHM (eV)		Height (Arb. Un.)	
Peak label	1 nm	bulk	1 nm	bulk	1 nm	bulk
C-H	284.29	284.29	0.62	0.62	0.82	0.82
C-1	284.66	284.66	0.72	0.71	0.32	0.35
C-2	285.48	285.48	0.71	0.71	0.34	0.31[a]
Shake-up C-H	286.08	286.08	0.76	0.76	0.06	0.04
Shake-up C-1	286.78	286.78	0.76	0.76	0.04	0.04
Shake-up C-2	287.28	287.28	0.76	0.76	0.04	0.03

[a]Beam damaged sample.

The fitting procedure reveals also the energy difference between the main feature and its associated shake-up. For each feature, both in the 1 nm thick film or in the bulk-like overlayer, the shake-up is found to be at 1.9 ± 0.2 eV higher binding energy than the corresponding main feature. This shake-up gives information on the molecular bandgap and agrees with already published results.[42,43]

Considering the results obtained on Si 2p and C 1s spectra, we can conclude that, as expected, there is no significant interaction between the molecules and Si atoms. Neither the N 1s spectrum (not presented here[44]) shows any differences between the line shape or energy positions between the thin and thick layers of $LuPc_2$. In general, both C 1s and N 1s spectra have similar line shapes to simple, single decker phthalocyanines,[13–15,41] indicating that the double molecular planes do not influence significantly the photoemission core lines. However, more insights into the electronic structure of this double decker Pc come from the absorption spectra and from the DFT simulations presented in Subsections IV B and IV C.

B. Experimental NEXAFS spectra

Figure 4 displays the NEXAFS spectra recorded with IPL (Fig. 4, red line) and OPL (Fig. 4, blue dashed line) with respect to the sample surface. Four different thicknesses are presented, i.e., from thin layer to bulk-like film (0.3 nm in (a), 1.5 nm in (b), 2.4 nm in (c), bulk in (d) being less than 10 nm). The features in the NEXAFS spectra of phthalocyanine molecular films at the N 1s edge are generated by electronic transitions from a core level to an unoccupied electronic level either with π or σ character. In the following part, we will use the convention that the azabridge nitrogen atoms are those connecting the pyrrole rings of the $LuPc_2$, while the pyrrole nitrogen atoms are those directly bonded to the lutetium atom in the central part of the rings. In the NEXAFS spectra of Pc films, the region where the $\pi^\star$ transitions are observed presents four main features that are labelled from A to D (peak A at around 398 eV, peak B at about 400 eV, peak C at about 403 eV and peak D at about 404 eV) as shown in spectrum (d) of Fig. 4. The broad absorption features at higher photon energies correspond to $\sigma^\star$ transitions (peaks E at around 407 eV and peak F at 409 eV, shown in spectrum (d) of Fig. 4). As for XPS results, no shifts in energy are observed with increasing thicknesses.

Information about the orientation of the molecules can be deduced from the relative intensities of the $\pi^\star$ and $\sigma^\star$ peaks in spectra taken at different orientations of the polarization vector E of the incident radiation with respect to the sample surface. Since $\pi^\star$ transitions dominate with OPL polarization, whereas $\sigma^\star$ transitions are dominant with IPL polarization, the molecules in films are found to lie rather flat on the surface at low coverages (spectra (a)–(c) in Fig. 4). The bulk spectra (Fig. 4(d)) show instead similar intensities for both $\sigma^\star$ and $\pi^\star$ resonances for the two incident polarizations (IPL and OPL). This can be ascribed either to a more tilted adsorption orientation of the molecules or to a less ordered overlayer, as will be further discussed in Sec. IV C dedicated to the theoretically simulated spectra.

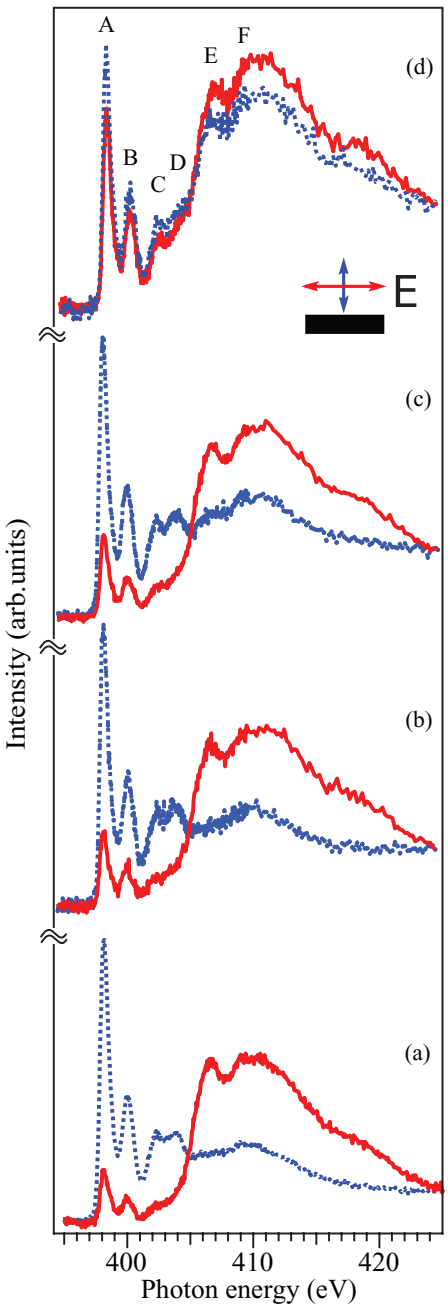

FIG. 4. NEXAFS spectra at the nitrogen 1*s* edge for incoming photons with in-plane polarization (red line) and out-of-plane polarization (blue dashed line); increasing thicknesses are displayed (a) 0.3 nm, (b) 1.5 nm, (c) 2.4 nm, and (d) bulk.

C. Theoretical NEXAFS spectra

The simulated absorption results, together with the experimental spectra for the 0.3 nm film and for the bulk layer, are presented in Fig. 5.

In part (i), we show a $\pi^\star$ resolved (I_π) calculation in comparison with the measured OPL spectrum of the 0.3 nm film. In part (ii), we show a $\sigma^\star$ resolved (I_σ) calculation in comparison with a measured IPL spectrum of the 0.3 nm film, and in part (iii) the theoretical simulation for a molecule adsorbed at a tilt angle θ of 45 °, in comparison with the measured OPL and IPL for the bulk film. The black curves are the total theoretical spectra, obtained by summing the pyrrole (red curve)

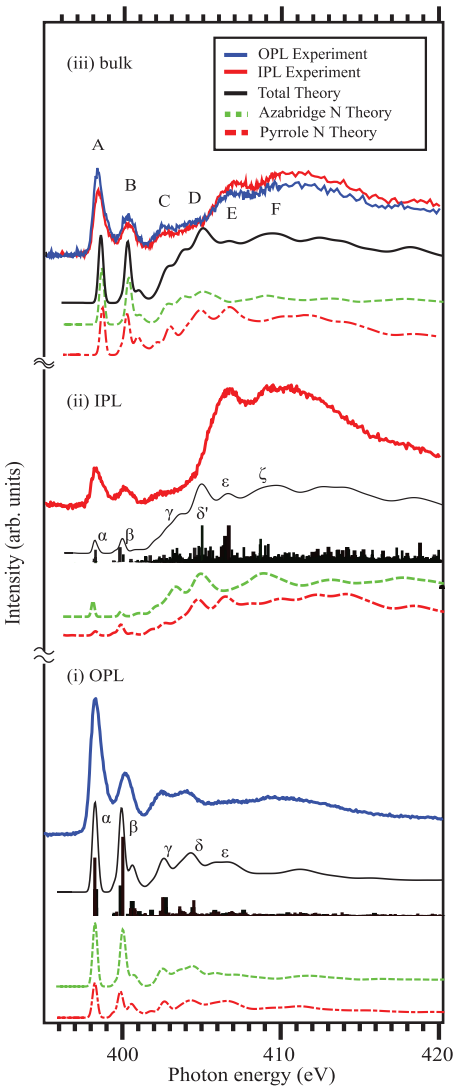

FIG. 5. Experimental and theoretical NEXAFS. (i) $\pi^\star$ resolved calculation and measurement for OPL polarization of a 0.3 nm thick film, (ii) $\sigma^\star$ resolved calculation and measurement of IPL polarization of a 0.3 nm thick film, (iii) calculation for $\theta = 45^\circ$ composed of $\pi^\star$ and $\sigma^\star$ calculation compared to bulk measurements; black curve shows total orientation resolved calculation; dashed red and green lines show pyrrole and azabridge N contributions, respectively; red and blue curves show measurements of the IPL and OPL polarizations.

and azabridge (green curve) nitrogen contributions. The bar graphs show the pDOS eigenvalues above HOMO obtained for both non-equivalent nitrogen species. In the total theoretical spectra of Fig. 5 (parts (i) and (ii)), the peaks labelled with greek letters from α to ζ with increasing energy have a good agreement with the experimental peaks A–F indicated in Fig. 4 and shown also in Fig. 5 (part (iii)).

The OPL calculation (Fig. 5, part (i)) is characterized by a number of resonances below 406 eV. The features α to δ of $\pi^\star$ character at about 398 eV, 400 eV, 403 eV, and 404 eV reproduce well the experimental peaks in the same energy region. The peaks C and D of the experiment, corresponding to Rydberg states, match well the γ and δ in the calculation.

The IPL calculations (Fig. 5, part (ii)) present very intense features above the photon energy of 406 eV, in the $\sigma^\star$ region which starts with a pronounced edge at about 407 eV. The theoretical $\sigma^\star$ resonances labelled ϵ and ζ are at 407 eV and at 409 eV. The peaks α and β are both clearly present in the IPL calculations and in the measured spectrum, and are very likely due to the non-planar geometry of the molecule. According to our computations, however, the different N species contribute with different intensities to these features. The intensity of the α peak is mainly due to the contribution of the azabridge nitrogen (green dashed curve), while the intensity of the β peak is mainly due to the contribution of the pyrrole nitrogen.

It is worth analyzing in more detail the origin of the α and β intensities in the spectra presented in Fig. 5, part (ii). Earlier NEXAFS studies on metal-phthalocyanines (M-Pc) have determined similar threshold peaks in IPL polarization measurements.[13] These peaks result from the interaction of the pyrrole N atoms with the metal center. In metal-free phthalocyanines, no such peaks were observed in the IPL polarization.[45] However, the structure of $LuPc_2$ is more complex than that of M-Pcs with a single Pc ring, due to the conjugation of two rings. One has to consider both the interaction between the metal and the Pc rings, and also the interaction of the two Pc rings with each other. For the OPL calculation, the intensities for each N species are similar, while for IPL α has mainly contributions from the azabridge N and β from the pyrrole N.

The spin resolved charge densities of the ground state displayed in Fig. 6 can give further information on the character of the first unoccupied molecular orbitals. We show the semi-unoccupied molecular orbital (SUMO) and SOMO and the LUMO for both spin states. The orbitals are delocalized over the whole molecule. The N atoms give only a small contribution to the HOMO (not shown here) and to the SUMO, while they contribute significantly to the LUMO and LUMO+1 (not shown here). Spin-up and spin-down LUMO have contributions from both the azabridge and pyrrole nitrogens, and from their neighboring carbon atoms. $\pi^\star$ like orbitals connect the two molecular rings in the spin-up LUMO and spin-down SUMO. In spin-up LUMO, there appears also some charge density originating from the interaction of the pyrrole N with the Lu atom. Our theoretical results indicate, therefore, that the Lu atom has influence on the low energy unoccupied levels: the interaction of the pyrrole atoms with the Lu leads to a partial occupation of the LUMO resulting in a lower intensity in the simulated NEXAFS spectra (red line in part (i) in Fig. 5). The low energy peaks also originate from the $\pi^\star$ like orbitals which extend between the two molecular rings.

Looking at the features at higher photon energies, one can observe that the theoretical features γ and δ are not in agreement with the IPL measurement (Fig. 5, part (ii)). The differences in intensity of the peaks δ in part (i) and δ' in part (ii), which are also slightly shifted in energy with respect to each other, can be ascribed to the limitation of the methods. GGA is known to contract states towards the Fermi level. It is known as well that the screening in σ and π states is different and the choice of a particular core-hole size[46] depends on the particular system. This effect has been described in previous studies.[46,47] In addition, effects like lifetime broadening and vibrations could also contribute to aberrations leading to the observed differences. In spite of these differences,

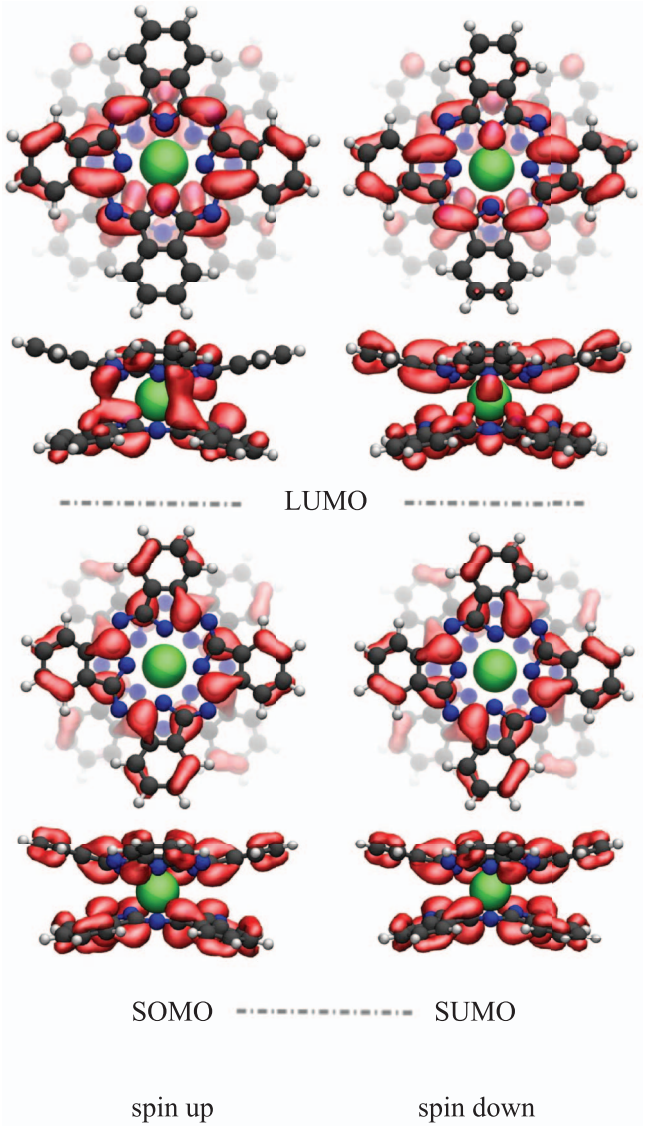

FIG. 6. Spin-up and spin-down charge densities obtained from the ground state calculations for SOMO/SUMO and LUMO, respectively. The same coloring of atoms was used as in Fig. 1.

the overall agreement between theory and experiment is very satisfactory. As mentioned previously, the NEXAFS spectra shown in Fig. 4 display a change of the molecular orientation between the thinner films (a)–(c) and the bulk (d). For the 0.3 nm film (a), we can assume adsorption parallel to the surface. This is also supported by the excellent agreement between theoretical and experimental results shown in Fig. 5 (parts (i) and (ii)). Moreover, the minor differences of the $\pi^\star$ and $\sigma^\star$ relative intensities observed in Figs. 4(a)–4(c) lead us to conclude that the molecules maintain about the same orientation for presented coverages. Instead, for the thick film, we note that the NEXAFS spectra in Fig. 4(d) show little difference in the relative $\pi^\star$ vs $\sigma^\star$ intensity ratio for the two polarizations. The little variation in intensities as a function of the polarization (observed in Fig. 4) can be ascribed to a molecular adsorption with an average tilt angle θ of approximately 45 ° confirmed by our theoretical calculation. In Fig. 5 (part (iii)) in fact we consider a superposition of $\pi^\star$ and $\sigma^\star$ states corresponding to an E-vector of the incident radiation forming an angle θ equal to 45 ° (considering the intensity ratios of peaks A and E). The total intensity I_{tot} at θ can be approximated then by $I_{tot}(45^\circ) = \cos^2(45^\circ)I_\pi + \sin^2(45^\circ)I_\sigma$. In this way, a 45 ° tilted molecule is simulated in the upper part of Fig. 5 (part (iii)). The very good agreement between the calculations and both bulk measurements for the IPL and OPL polarizations up to 407 eV leads us to suggest a staggering of the molecules close to 45 °. However, it is important to mention that similar results regarding the relative $\pi^\star$ vs $\sigma^\star$ intensities at different acquisition geometries can be due to a disordered film. To answer this question, additional studies need to be carried out. A promising tool for such studies would be Reflectance Anisotropy Spectroscopy (RAS) measurements that have been carried out previously on similar systems.[11]

V. CONCLUSIONS

We have measured the Si 2p and the C 1s XPS and N 1s NEXAFS on films of $LuPc_2$ with increasing thickness from 0.2 nm to bulk-like films adsorbed on a passivated Si(100)2 × 1 reconstructed vicinal surface. The photoelectron spectroscopy results confirm that the $LuPc_2$ films do not interact significantly with the H-passivated Si substrate indicating that the presented results describe well the molecular electronic structure. The NEXAFS measurements show that the molecules in the films undergo an increase in average tilt angle with respect to the sample surface. Our theoretical DFT simulations evidence that $LuPc_2$ molecules in the film at the lowest thickness lie flat on the surface and reach a maximum average tilt angle θ of about 45 ° in the thicker film. Our experimental findings suggest that the films are predominantly ordered for low coverages (up to several nm) but, for thicker layers, additional investigations are needed to determine the actual proportion of the ordered molecules and their tilt angle. The DFT calculations suggest that the threshold features observed in the IPL measurement result as a consequence of the molecular bent structure and of the interaction between the two phthalocyanine rings and the lutetium metal center.

ACKNOWLEDGMENTS

We are grateful to Knut and Alice Wallenbergs Foundation (KAW) for financial support. The Swedish National Infrastructure for Computing (SNIC) has provided computing time on the clusters Akka at Umeå University and Neolith at Linköping University. B.B., C.P., O.E., and J.R. acknowledge the Swedish Research Council. Images of the atomic structures were made using VMD.[48] C.G. is grateful to the TALENTS Programme (7th R&D Framework Programme, Specific Programme: PEOPLE – Marie Curie Actions – COFUND) for financial support.

[1] L. Carrette, K. A. Friedrich, and U. Stimming, Chem. Phys. Chem. **1**, 162 (2000).
[2] M. Thelakkat, C. Schmitz, and H.-W. Schmidt, Adv. Mater. **14**, 577 (2002).
[3] G. Guillaud, M. A. Sadoun, M. Maitrot, J. Simon, and M. Bouvet, Chem. Phys. Lett. **167**, 503 (1990).
[4] Y. Chen, D. Li, N. Yan, J. Gao, R. Gu, G. Lu, and M. Bouvet, J. Mater. Chem. **22**, 22142 (2012).

[5]V. Parra, M. Bouvet, J. Brunet, M. L. Rodríguez-Méndez, and J. A. de Saja, Thin Solid Films **516**, 9012 (2008).
[6]J. Brunet, V. P. Garcia, A. Pauly, C. Varenne, and B. Lauron, Sens. Actuators B **134**, 632 (2008).
[7]J. D. Baran, J. A. Larsson, R. A. J. Woolley, Y. Cong, P. J. Moriarty, A. A. Cafolla, K. Schulte, and V. R. Dhanak, Phys. Rev. B **81**, 075413 (2010).
[8]K. Nilson, J. Åhlund, M.-N. Shariati, E. Göthelid, P. Palmgren, J. Schiessling, S. Berner, N. Mårtensson, and C. Puglia, J. Phys. Chem. C **114**, 12166 (2010).
[9]E. Salomon, N. Papageorgiou, T. Angot, A. Verdini, A. Cossaro, L. Floreano, A. Morgante, L. Giovanelli, and G. Le Lay, J. Phys. Chem. C **111**, 12467 (2007).
[10]R. P. Berkelaar, H. Sode, T. F. Mocking, A. Kumar, B. Poelsema, and H. J. W. Zandvliet, J. Phys. Chem. C **115**, 2268 (2011).
[11]S. Boudet, I. Bidermane, E. Lacaze, B. Gallas, M. Bouvet, J. Brunet, A. Pauly, Y. Borensztein, and N. Witkowski, Phys. Rev. B **86**, 115413 (2012).
[12]F. Seidel, M. Fronk, C. Himcinschi, V. Chis, and D. R. T. Zahn, Phys. Status Solidi C **7**, 222 (2010).
[13]J. Ahlund, K. Nilson, J. Schiessling, L. Kjeldgaard, S. Berner, N. Martensson, C. Puglia, B. Brena, M. Nyberg, and Y. Luo, J. Chem. Phys. **125**, 034709 (2006).
[14]L. Wang, D. Qi, L. Liu, S. Chen, X. Gao, and A. T. S. Wee, J. Phys. Chem. C **111**, 3454 (2007).
[15]B. N. Holland, G. Gavrila, D. R. T. Zahn, A. A. Cafolla, C. McGuinness, and I. T. McGovern, Phys. Status Solidi C **7**, 218 (2010).
[16]J. Gardener, J. Owen, K. Miki, and S. Heutz, Surf. Sci. **602**, 843 (2008).
[17]Y. Borensztein and N. Witkowski, J. Phys. Condens. Matter **16**, S4301 (2004).
[18]N. Witkowski, R. Coustel, O. Pluchery, and Y. Borensztein, Surf. Sci. **600**, 5142 (2006).
[19]J. Boland, Surf. Sci. **261**, 17 (1992).
[20]M. Bouvet and J. Simon, Chem. Phys. Lett. **172**, 299 (1990).
[21]S. Hufner, *Photoelectron Spectroscopy: Principles and Applications*, 2nd ed. (Springer-Verlag, 1996), pp. 12–13.
[22]F. Polack, M. Silly, C. Chauvet, B. Lagarde, N. Bergeard, M. Izquierdo, O. Chubar, D. Krizmancic, M. Ribbens, J. P. Duval, C. Basset, S. Kubsky, and F. Sirotti, AIP Conf. Proc. **1234**, 185 (2010).
[23]D. A. Shirley, Phys. Rev. B **5**, 4709 (1972).
[24]C. Mathieu, X. Bai, J. J. Gallet, F. Bournel, S. Carniato, F. Rochet, E. Magnano, F. Bondino, R. Funke, U. Kohler, and S. Kubsky, J. Phys. Chem. C **113**, 11336 (2009).
[25]R. Denecke, P. Väterlein, M. Bässler, N. Wassdahl, S. Butorin, A. Nilsson, J. E. Rubensson, J. Nordgren, N. Mårtensson, and R. Nyholm, J. Electron Spectrosc. Relat. Phenom. **101**, 971 (1999).
[26]J. Stöhr, *NEXAFS Spectroscopy*, Springer Series in Surface Sciences Vol. 25 (Springer, 2003), pp. 154–161.
[27]M. J. Frisch, G. W. Trucks, H. B. Schlegel *et al.*, GAUSSIAN 09, Revision A.1, Gaussian, Inc., Wallingford, CT, 2009; found online at http://www.gaussian.com/g_tech/g_ur/m_citation.htm.
[28]A. D. Becke, J. Chem. Phys. **98**, 1372 (1993).
[29]J. Yang and M. Dolg, Theor. Chem. Acc. **113**, 212 (2005).
[30]A. De Cian, M. Moussavi, J. Fisher, and R. Weiss, Inorg. Chem. **24**, 3162 (1985).
[31]R. Murdey, M. Bouvet, M. Sumimoto, S. Sakaki, and N. Sato, Synth. Met. **159**, 1677 (2009).
[32]T. Yanai, D. P. Tew, and N. C. Handy, Chem. Phys. Lett. **393**, 51 (2004).
[33]J. C. Slater, Adv. Quantum Chem. **6**, 1 (1972).
[34]J. C. Slater and K. H. Johnsson, Phys. Rev. B **5**, 844 (1972).
[35]L. Triguero, Y. Luo, L. G. M. Pettersson, H. Agren, P. Väterlein, M. Weinelt, A. Föhlisch, J. Hasselström, O. Karis, and A. Nilsson, Phys. Rev. B **59**, 5189 (1999).
[36]P. Blaha, K. Schwarz, G. K. H. Madsen, D. Kvasnicka, and J. Luitz, WIEN2k, an augmented plane wave + local orbitals program for calculating crystal properties, Techn. Universität Wien, Austria, 2001.
[37]J. P. Perdew, M. Ernzerhof, and K. Burke, J. Chem. Phys. **105**, 9982 (1996).
[38]C. Mathieu, X. Bai, F. Bournel, J.-J. Gallet, S. Carniato, F. Rochet, F. Sirotti, M. G. Silly, C. Chauvet, D. Krizmancic, and F. Hennies, Phys. Rev. B **79**, 205317 (2009).
[39]R. Uhrberg, E. Landemark, and Y.-C. Chao, J. Electron. Spectrosc. Relat. Phenom. **75**, 197 (1995).
[40]H. W. Yeom, H. Hamamatsu, T. Ohta, and R. I. G. Uhrberg, Phys. Rev. B **59**, R10413 (1999).
[41]M. Toader, M. Knupfer, D. R. T. Zahn, and M. Hietschold, J. Am. Chem. Soc. **133**, 5538 (2011).
[42]L. Smykalla, P. Shukrynau, and M. Hietschold, J. Phys. Chem. C **116**, 8008 (2012).
[43]B. Brena, Y. Luo, M. Nyberg, S. Carniato, K. Nilson, Y. Alfredsson, J. Ahlund, N. Martensson, H. Siegbahn, and C. Puglia, Phys. Rev. B **70**, 195214 (2004).
[44]See supplementary material at http://dx.doi.org/10.1063/1.4809725 for comparison of nitrogen 1s spectra.
[45]Y. Alfredsson, B. Brena, K. Nilson, J. Åhlund, and L. Kjeldgaard, J. Chem. Phys. **122**, 214723 (2005).
[46]R. Laskowski, T. Gallauner, P. Blaha, and K. Schwarz, J. Phys.: Condens. Matter **21**, 104210 (2009).
[47]M. Nyberg, Y. Luo, L. Triguero, L. G. M. Pettersson, and H. Agren, Phys. Rev. B **60**, 7956 (1999).
[48]W. Humphrey, A. Dalke, and K. Schulten, J. Mol. Graphics Modell. **14**, 33 (1996).